RSC Advances

PAPER

View Article Online
View Journal | View Issue

Cite this: *RSC Adv.*, 2020, **10**, 2428

Formulation of a graft polymer-containing aqueous yellow ceramic ink for digital ink-jet printing

Ji-Hyeon Lee,[a] Jin-Ho Kim,[a] Kwang-Taek Hwang,[a] Hae-Jin Hwang[b] and Kyu-Sung Han *[a]

Received 18th November 2019
Accepted 26th December 2019

DOI: 10.1039/c9ra09595k

rsc.li/rsc-advances

We herein reported the preparation of an eco-friendly aqueous yellow ceramic ink and subsequent examination of its printability for ink-jet printing applications. For this purpose, a water based ceramic ink was formulated using ceramic pigments to give a clear color during high-temperature heat treatment (>1000 °C), ultimately yielding an ink suitable for application in ceramic tile decoration. To improve the low dispersion stability of the aqueous ceramic ink compared to that of a conventional organic solvent-based ceramic ink, the pigment particles were dispersed using a graft polymer. More specifically, this graft polymer was composed of polyacrylic acid as the main chain to provide electrostatic repulsion and grafted poly(ethylene glycol) methyl ether methacrylate as the side chain to provide steric hindrance. Furthermore, additive-induced foaming issues were significantly reduced through the use of this graft polymer as a surfactant. The effects of the rheological properties of the prepared ceramic ink and the subsequent operation conditions of the piezoelectric print head were then investigated in detail to optimize the ink jettability and printability.

Introduction

Digital ink-jet printing is a technology based on sending digitized pattern data to an ink-jet printer and jetting ink droplets to directly print the pattern on a substrate.[1,2] This digital ink-jet printing technology has a number of advantages compared to conventional graphic printing technologies. The digital ink-jet printing process can easily create or customize the printing image, and no contact is necessary between the substrate and the print head, thereby allowing various materials and complex-shaped objects to be used as substrates. In addition, due to the ink being jetted only onto the desired location using the drop on demand (DoD)-based digital ink-jet printing method, this printing technique can achieve a high ink efficiency.[3–6]

Due to these advantages, ceramic ink-jet printing has become the technology of choice over the past decade in the ceramic tile decoration industry. However, despite its success, this industry has recently been faced with the pressure of environmental issues such as global warming and air pollution.[7] Since the majority of inks employed in digital ink-jet printing are based on organic solvents and contain volatile organic compounds (VOCs) to ensure their dispersion stability and printability, the development of eco-friendly and functional ceramic inks to replace VOC-containing organic solvent-based ink-jet printing inks is required.[8,9]

As such, the physical properties of existing ceramic inks must be satisfied to ensure successful ink-jet printing for the decoration of ceramic tiles.[10–13] In this context, the ceramic pigments present in ceramic ink must be thermally stable to ensure that the desired color is maintained at sintering temperatures >1000 °C. In addition, the pigment particles should show an appropriate particle size distribution and a high dispersion stability to prevent nozzle clogging of the ink-jet printer head.[14] Furthermore, the rheological properties of the ceramic ink, such as the viscosity and surface tension, must be optimized along with the print head voltage and pulse width to ensure that spherical-shaped single ink droplets are formed without undesirable satellite droplets.[15,16]

Thus, we herein report the formulation of an eco-friendly aqueous ceramic ink for digital ink-jet printing and subsequent examination of its ink-jet printability. For this purpose, thermally stable ceramic pigments are dispersed in an aqueous solution using a graft polymer as a surfactant. The jetting behavior and printing characteristics of the synthesized aqueous ceramic ink are then investigated in detail upon variation in the rheological properties of the ceramic ink and the operating conditions of the ink-jet print head.

Experimental section

Preparation of the yellow ceramic pigments

Yellow ceramic pigments of Pr–$ZrSiO_4$ were synthesized using a solid-state reaction process.[17] The solid-state reaction process is a synthesis method using ionic or atomic diffusion

[a]*Korea Institute of Ceramic Engineering and Technology, Icheon Branch, Icheon 17303, Republic of Korea. E-mail: kh389@kicet.re.kr*
[b]*Division of Material Science and Engineering, Inha University, Incheon 22212, Republic of Korea*

phenomena, which occurs on the adjacent surfaces between particles, in a high-temperature environment after mixing materials such as oxides or carbonates. As starting materials for synthesis of the ceramic pigments, ZrO_2 (Sigma Aldrich), SiO_2 (Showa), and Pr_6O_{11} (Sigma Aldrich) were used. Additionally, NaF (Sigma Aldrich) was used as a mineralizer. The synthesis of $ZrSiO_4$ is started with the initial reaction occurs between SiO_2 and the mineralizer which produces a volatile species.[18]

$$SiO_2 + 4NaF \rightarrow SiF_4\,(g) + 2Na_2O \quad (1)$$

$$SiF_4 \rightarrow Si^{4+} + 4e^- + 2F_2 \quad (2)$$

$$Si^{4+} + 4e^- + ZrO_2 + O_2 \rightarrow ZrSiO_4 \quad (3)$$

The Pr exists as a dopant and trivalent state in the melt phase of the mixture at 260–300 °C. Then, it is transformed into tetravalent state at the higher temperature and incorporated into the $ZrSiO_4$ structure of the pigment.[19] The starting materials (60 wt% ZrO_2, 35 wt% SiO_2, 5 wt% Pr_6O_{11}) and the mineralizer (3 wt% to the mixture of the starting materials) were wet mixed for 3 h with alumina balls and ethanol, and after this time, the mixed powder was dried at 80 °C in an oven, then sintered at 1100 °C for 1 h under an oxidizing atmosphere. The resulting yellow ceramic pigments were then micronized using a bead mill (KMD-1S, Dntech, Korea) to prevent nozzle clogging of the ink-jet print head. The crystal structure of the pigment was analyzed by X-ray diffraction (XRD, D/2500VL/PC, Rigaku, Japan). Field emission scanning electron microscopy (FE-SEM, JSM-6390, Jeol, Japan) and particle size analysis (PSA, LA-950V2, Horiba, Japan) were carried out to analyze the morphology and particle size distribution.

Formulation of the aqueous yellow ceramic ink

The aqueous yellow ceramic ink was formulated by mixing distilled water and 15 vol% of the yellow ceramic pigment. The dispersion stability of the aqueous ceramic ink was characterized upon the addition of sodium dodecyl sulfate (SDS, Sigma Aldrich), polyacrylic acid (PAA, M_w 1800, Sigma Aldrich), poly(-ethylene glycol) methyl ether methacrylate (PMEM, M_w 950, Sigma Aldrich), or PAA-*g*-PMEM, in which PAA was grafted with PMEM. The surfactants were added to the ceramic ink within the ranges of 0–1.0 mg m^{-2}. To adjust the rheological properties of the aqueous ceramic ink, 0–15 wt% polyethylene glycol (PEG, M_w 8100, Sigma Aldrich) was added as a thickener and 0–0.1 wt% polysiloxane (BYK-028, BYK) was added as a surface tension modifier. A rotational rheometer (HAAKE MARS III, Thermo Fisher Scientific, USA) and surface tension analyzer (DST-60, Surface Electro Optics, Korea) were used to measure the viscosity and surface tension of the aqueous ceramic ink, respectively. The sedimentation behavior and dispersion stability of the pigment particles in the ceramic ink were analyzed quantitatively using Turbiscan (Turbiscan LAB, Formulaction, France). The hydrodynamic radius and surface charge of the pigment particles were analyzed using a particle size analyzer (VASCO, Cordouan, France) and a zeta potential analyzer (ELS-Z, Otsuka Electronics, Japan), respectively.

Synthesis of the graft polymer surfactant

PAA, PMEM, ammonium persulfate (APS, Samchun) and hydroquinone monomethyl ether (MEHQ, Samchun) were used for the synthesis of graft polymer surfactant. PAA and PMEM (PAA/PMEM molar ratio = 2.0) with MEHQ (1.0 wt% to the total weight of monomers) were mixed in DI water. After being fully dissolved, PAA solution and APS (0.5 wt% to the total weight of monomers) were added drop-wise into the DI water in a reactor. The reactor equipped with a reflux condenser, feeding inlets and gas inlet tube. The mixture was stirred and heated at 85 °C for 5 h. Afterwards, the reacted solution was cooled to room temperature, the pH value was adjusted to 5.5 with NaOH (50 wt% aqueous solution). Finally, a brown and clear graft polymer surfactant (20 wt% of solid content in aqueous solution) was obtained.[20]

Printability analysis of the prepared aqueous yellow ceramic ink

The printability of the aqueous ceramic ink was determined using a drop watcher (Omnijet 450, Unijet, Korea), which had a piezoelectric ink-jet print head with a 48 μm nozzle diameter. The waveform of the piezoelectric print head employed a single pulse voltage pattern. The voltage and pulse width of the waveform were set within the ranges of 70–90 V and 6–10 μs, respectively. The rising time and fall time were set as 3 μs. The aqueous ceramic ink was printed on a ceramic tile substrate with a distance between printed dots (D2D, drop to drop) of 200 μm. The shape factor of the printed dots was then calculated to evaluate the printing quality, where the area and perimeter of the printed dots were analyzed using image analysis software (Image J, National Institute of Health, USA).

$$\text{Shape factor} = \frac{4\pi(\text{area})}{(\text{perimeter})^2} \quad (4)$$

In this context, we note that the shape factor of a circular dot is close to 1, while the shape factor of a linear dot is close to 0.[21,22]

Results and discussion

Characterizations of the yellow ceramic pigment

The crystal structure, morphology, and particle size of the synthesized yellow ceramic pigments obtained after milling were investigated. The crystal structure of the yellow ceramic pigment used in this study is a Pr doped $ZrSiO_4$. $ZrSiO_4$ has a principal structural unit of edge-sharing SiO_4 tetrahedra and ZrO_8 triangular dodecahedra which contains the empty octahedral void.[23] Pr^{4+} generated by a Pr dopant is accommodated into both Zr^{4+} and Si^{4+} sites of the $ZrSiO_4$ lattice, it imparts the yellow color of the ceramic pigment.[24] Fig. 1a showed the XRD pattern of the yellow ceramic pigment that confirmed the presence of $ZrSiO_4$ phase (JCPDS no. 01-080-1807) as the main phase of the ceramic pigment, although small peaks corresponding to unreacted ZrO_2 (JCPDS no. 03-065-0687) were also observed. Fig. 1b shows the morphology and particle size of

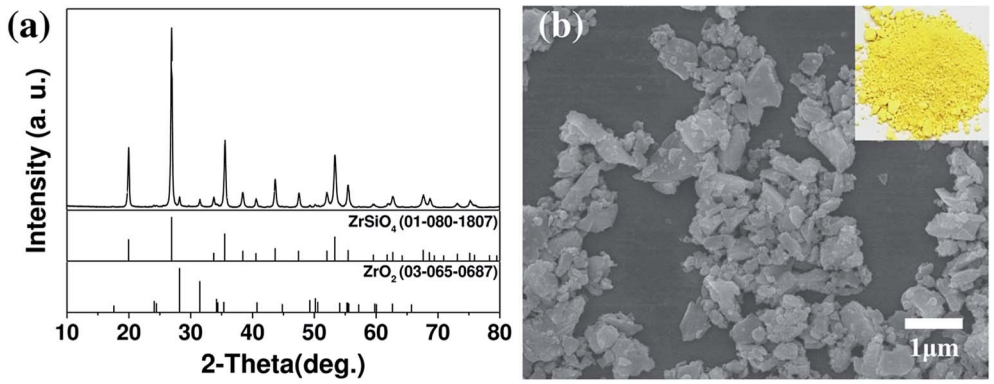

Fig. 1 (a) XRD pattern, and (b) FE-SEM image of the yellow ceramic pigments. Inset shows an optical image of the pigment powder.

micronized ceramic pigment which are important variables for ink-jet printing application. Based on the FE-SEM image, the particle size of micronized yellow ceramic pigment was approximately 50–900 nm. The morphology of ceramic pigment seemed irregular particle shape with rough edges. This shape of micronized ceramic pigment particle is due to a broken down of the ceramic particle by a high mechanical energy during the micronization process. In terms of the morphology and particle size, to prevent nozzle clogging in the ink-jet print head, the largest particle size should be 1/50 of the print head nozzle diameter, and the average particle size should be smaller than 300 nm.[14,25,26] Thus, the D_{90} value and the average particle size of the micronized ceramic pigments employed herein were found to be 647 and 298 nm respectively.

Preparation of the aqueous yellow ceramic ink for ink-jet printing

Yellow ceramic ink was formulated by mixing with distilled water and 15 vol% of the yellow ceramic pigment. In an aqueous solution, agglomeration of the ceramic particles can easily occur, thereby leading to nozzle clogging during ink-jet printing. To address this issue, a graft polymer, namely PAA-*g*-PMEM, was added as a dispersant. In this graft polymer, the

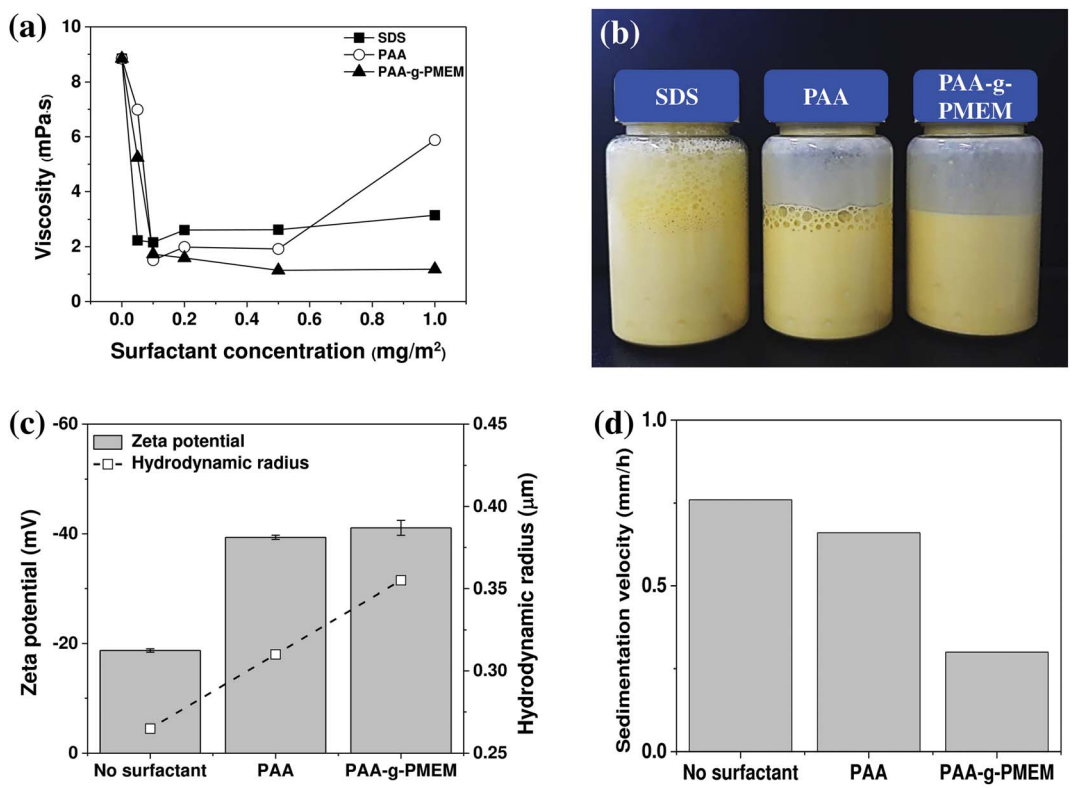

Fig. 2 (a) Viscosity, (b) foaming behavior, (c) zeta potential and hydrodynamic radius, and (d) sedimentation velocity of the aqueous ceramic ink in the absence of surfactant and in the presence of PAA and PAA-*g*-PMEM.

PAA main chain was selected to ensure electrostatic repulsion and the PMEM side chain was chosen to impart steric hindrance. It is expected that a high dispersion stability of pigment particles in the aqueous ceramic ink can be achieved when the effects of electrostatic repulsion and steric hindrance are combined.[20,27–29] Thus, Fig. 2a shows a comparison of the viscosities of the aqueous ceramic ink samples in the presence of the SDS, PAA, and PAA-*g*-PMEM surfactants, where the viscosity depends on interactions between the particles. More specifically, weak interactions lead to a low viscosity, while strong interactions lead to a high viscosity. Hence, the lower viscosity observed upon the addition of a surfactant indicates an improvement in the dispersion stability.[30–32] Regardless of the surfactant type employed, the viscosity of the aqueous ceramic ink initially decreased upon increasing the surfactant concentration, and the lowest viscosity of 1.14 mPa s was observed in the aqueous ceramic ink sample containing 0.5 mg m^{-2} PAA-*g*-PMEM. This value represents the optimal surfactant concentration to ensure sufficient adsorption onto the ceramic particle surface, thereby effectively hindering the interaction between ceramic particles. However, in the presence of excess adsorbed surfactant, bridging or entanglement occurs and the viscosity of the ceramic ink increases.[33,34]

The foaming behavior was then investigated upon the addition of SDS, PAA, and PAA-*g*-PMEM to the aqueous ceramic ink (Fig. 2b). In general, large amounts of foam can form when a surfactant is added to a water-based suspension, and the presence of such a microfoam in the aqueous ceramic ink may interrupt the ink flow through the nozzle or channel of the ink-jet print head. Interestingly, we found that foaming did not occur after mixing of the aqueous ceramic ink with PAA-*g*-PMEM, although for SDS and PAA, it was apparent that an additional defoaming agent would be required.

Subsequently, the dispersion stability of the aqueous ceramic ink was examined, where Fig. 2c shows the results of the zeta potential and hydrodynamic radii investigations. In the absence of a surfactant, the zeta potential of the aqueous ceramic ink was −18.7 mV, while upon the addition of PAA and PAA-*g*-PMEM, the zeta potentials were −39.4 and −41.1 mV, respectively, thereby indicating an improvement in the dispersion stability. Generally, a zeta potential between 0 and ±30 mV is considered to represent a low dispersion stability, while values over ±30 mV indicate a good dispersion stability.[35,36]

The hydrodynamic radius was also calculated using the following Stokes–Einstein equation:[37,38]

$$R = \frac{kT}{6\pi\eta D} \quad (5)$$

where D is the diffusion coefficient, k is the Boltzmann constant, T is the temperature, η is the viscosity, and R is the hydrodynamic radius. In the case of the ceramic pigment particles, a thick hydrodynamic radius tends to give a ceramic ink with a long-lasting dispersion stability.[39,40] In this case, the hydrodynamic radius of the aqueous ceramic ink in the absence of a surfactant was 265 nm, while in the presence of PAA and PAA-*g*-PMEM, values of 310 and 355 nm were determined, respectively. The higher zeta potentials and hydrodynamic radii obtained in the presence of the PAA and PAA-*g*-PMEM surfactants were attributed to the effect of PAA, although slightly superior values being obtained upon the grafting of PMEM due to the enhanced steric barrier on the pigment particle surface.

The sedimentation velocities of the aqueous ceramic inks in the presence of PAA and PAA-*g*-PMEM were then examined, as displayed in Fig. 2d. In this case, similar values were obtained for the samples containing no surfactant and containing PAA (*i.e.*, 0.76 and 0.66 mm h^{-1}, respectively). In contrast, PAA-*g*-PMEM addition significantly decreased the sedimentation velocity to 0.30 mm h^{-1}, which is 55% slower than that of the PAA-containing sample.

In the ink-jet printing process, the physical properties of the ceramic ink (*e.g.*, viscosity and surface tension) strongly influence the jetting behavior of the ink droplets. For example, a high viscosity and surface tension can increase the system pressure, while a low viscosity and surface tension cause undesirable ink dripping and spreading over the print head nozzle.[1,41,42] Thus, the jetting behavior of a fluid can be determined in terms of the Ohnesorge number (Oh) of the ink. The inverse values of the Ohnesorge number (Z) for the aqueous ceramic inks were thus determined based on their rheological properties (see Table 1) according to the following equation:

$$Z = \mathrm{Oh}^{-1} = \frac{\sqrt{\rho\gamma L}}{\eta} \quad (6)$$

where η is the viscosity, ρ is the density, γ is the surface tension, and L is the characteristic length scale.[43] It was suggested that a Z value of ink within the range of 1 and 10 is required for

Table 1 Inverse values of the Ohnesorge number for aqueous yellow ceramic inks exhibiting various rheological properties

Thickener (wt%)	Surface tension modifier (wt%)	Viscosity (mPa s)	Surface tension (mN m^{-1})	Inverse of ohnesorge number (Z)
0	0	1.1	63.4	56.8
5	0	3.5	63.4	18.8
10	0	5.3	63.4	12.3
15	0	10.4	63.4	6.2
15	0.005	10.4	44.3	5.2
15	0.01	10.4	42.5	5.1
15	0.1	10.4	38.7	4.9

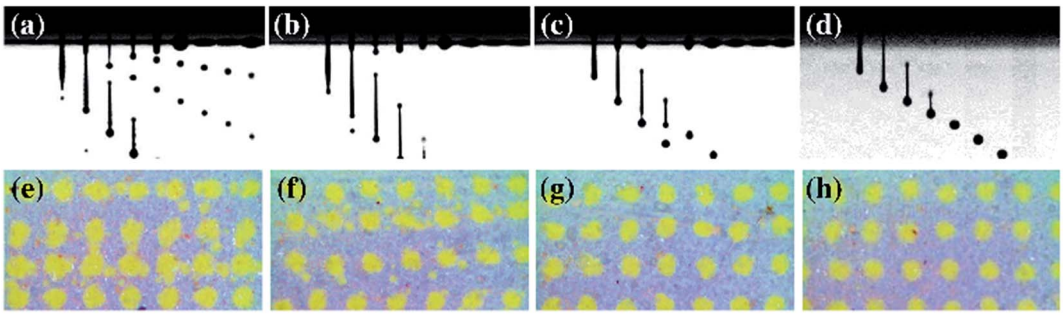

Fig. 3 Drop formation for the aqueous yellow ceramic ink containing thickener concentrations of (a) 0 wt%, (b) 5 wt%, (c) 10 wt%, and (d) 15 wt%. Corresponding printed dot images of the aqueous yellow ceramic ink containing thickener concentrations of (e) 0 wt%, (f) 5 wt%, (g) 10 wt%, and (h) 15 wt%.

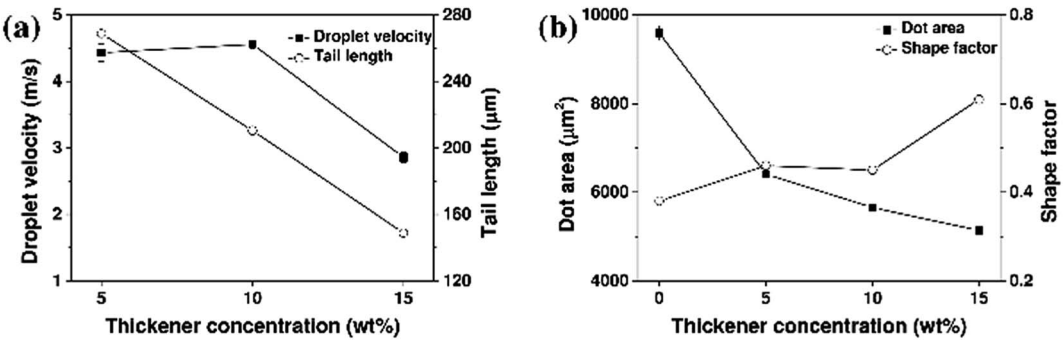

Fig. 4 (a) Droplet velocities, and (b) dot areas of the aqueous yellow ceramic ink containing a range of thickener concentrations.

suitable jetting. A low Z value caused by a high viscosity requires a high pulse pressure for jetting, and a high Z value results in both lengthening of the droplet tail and the generation of satellite droplets.[44] The Z value of the initial aqueous ceramic ink was 56.8 due to the low viscosity and high surface tension of water. Upon the addition of a thickener, the Z value gradually decreased due to an increased ink viscosity. The addition of 15 wt% thickener gave a Z value of 6.2, which is suitable for ink-jet printing. It should also be noted that a reduction in the surface tension through the addition of a surface tension modifier was found to give a slightly lower Z value.

Ink-jet printability of the aqueous yellow ceramic ink

The jetting behavior and printability of the aqueous ceramic inks with different viscosities were then examined as displayed in Fig. 3 and 4. Prior to adjustment of the rheological properties, a long droplet tail and satellite droplets were observed, and dripping was also found after jetting of the initial ink droplet. As such, a low shape factor and a large dot area resulted. Upon increasing the viscosity of the aqueous ceramic ink through the addition of a thickener, satellite droplet generation was reduced, and the ink droplet velocity and droplet tail length decreased. The droplet velocity and tail length results obtained prior to adjustment of the rheological conditions have been

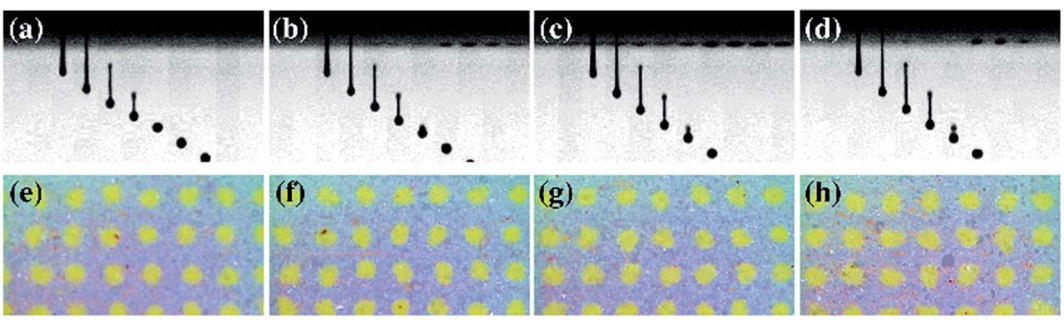

Fig. 5 Drop formation for the aqueous yellow ceramic ink containing surface tension modifier concentrations of (a) 0 wt%, (b) 0.005 wt%, (c) 0.01 wt%, and (d) 0.1 wt%. Corresponding printed dot images of the aqueous yellow ceramic ink containing surface tension modifier concentrations of (e) 0 wt%, (f) 0.005 wt%, (g) 0.01 wt%, and (h) 0.1 wt%.

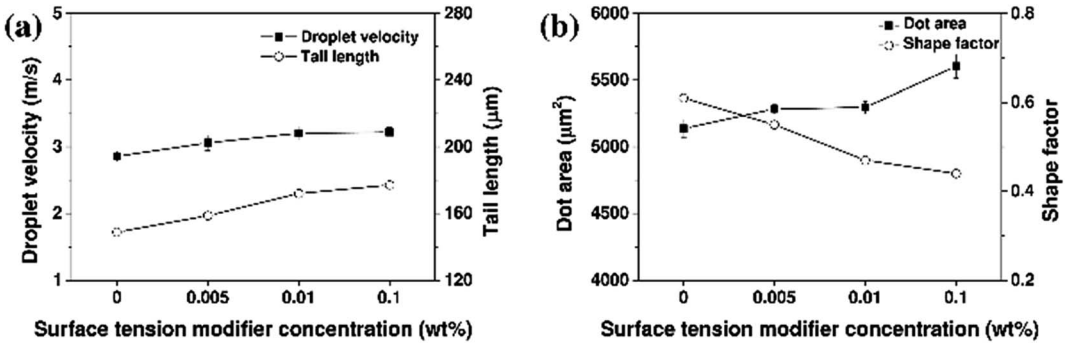

Fig. 6 (a) Droplet velocities, and (b) dot areas for the aqueous yellow ceramic ink containing different concentrations of surface tension modifier.

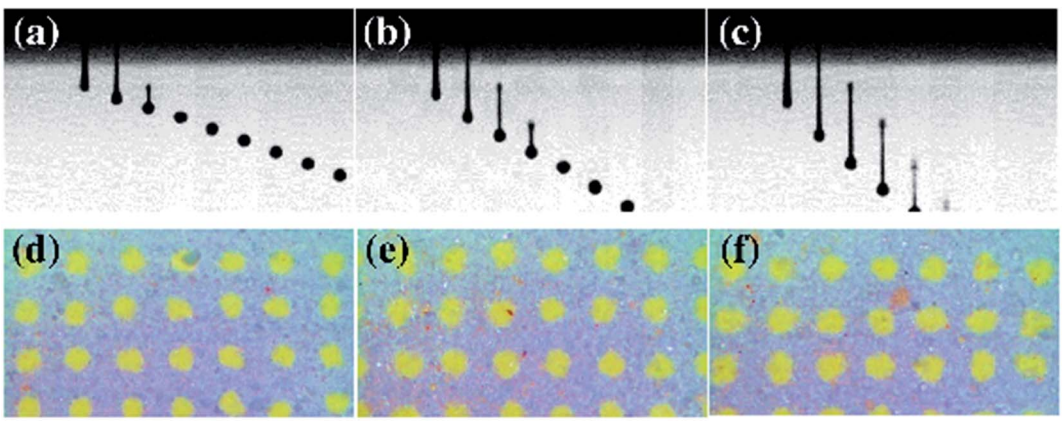

Fig. 7 Drop formation for the aqueous yellow ceramic ink with input voltages of (a) 70 V, (b) 80 V, and (c) 90 V. Corresponding printed dot images of the aqueous yellow ceramic ink with input voltages of (d) 70 V, (e) 80 V, and (f) 90 V.

omitted due to the large numbers of satellite droplets observed. Thus, upon improving the jettability of the ink by increasing the viscosity, the printed dot area decreased and the shape factor improved. These results therefore indicate that the viscosity influenced the flow resistance of the aqueous ceramic ink, with an appropriate level of flow resistance being necessary to give an optimal printing quality.[45]

Fig. 5 and 6 show the jetting behavior and printability results for the aqueous ceramic inks of different surface tensions. To analyze the effect of surface tension modification on the printability, the thickener concentration was fixed at 15 wt%. No satellite droplets were observed regardless of the added quantity of surface tension modifier. However, upon increasing the surface tension modifier content, the droplet velocity and droplet tail length of the aqueous ceramic ink also increased. It should be noted that a high surface tension in the ceramic ink imparts flow resistance in the ink-jet printing process; as the surface tension modifier concentration was

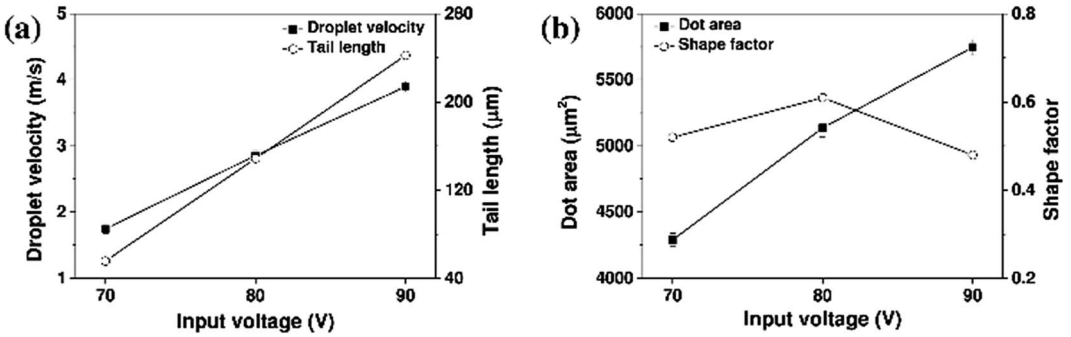

Fig. 8 (a) Droplet velocities, and (b) dot areas of the aqueous yellow ceramic ink with different print head input voltages.

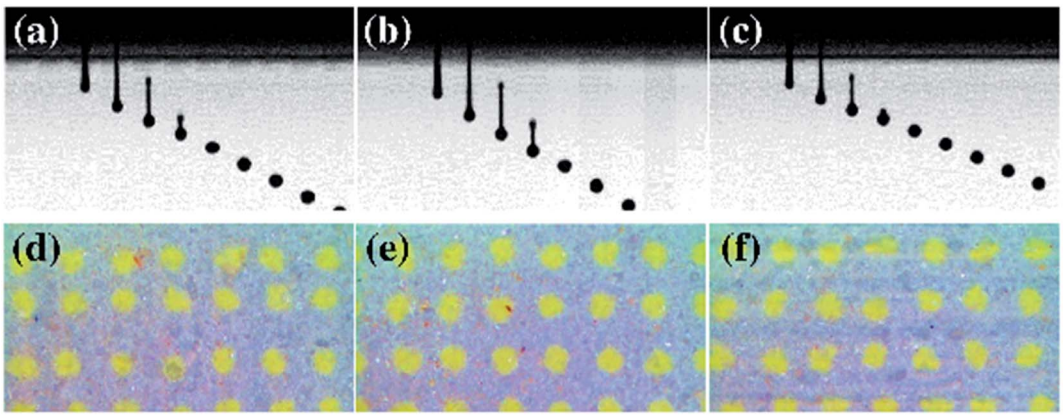

Fig. 9 Drop formation for the aqueous ceramic ink with pulse widths of (a) 6 μs, (b) 8 μs, and (c) 10 μs. Corresponding printed dot images of the aqueous ceramic ink with pulse widths of (d) 6 μs, (e) 8 μs, and (f) 10 μs.

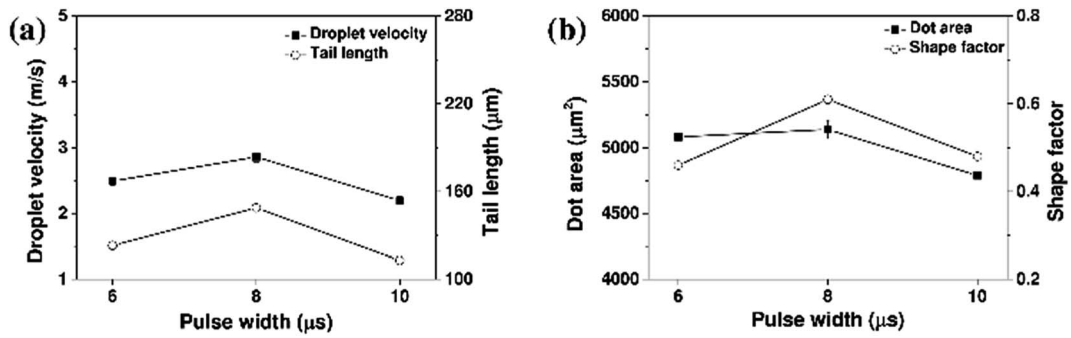

Fig. 10 (a) Droplet velocities, and (b) dot areas of the aqueous yellow ceramic ink with different print head pulse widths.

increased, the droplet velocity increased due to a decrease in the flow resistance. In addition, when ink droplets with a high surface tension are exposed to air, the droplets quickly form a spherical shape by reducing the surface area to lower the surface tension, thereby leading to a shorter tail length and a delay in spherical droplet formation.[46,47] Furthermore, an increase in the surface tension modifier concentration resulted in the dot area of the aqueous ceramic ink on a ceramic substrate increasing, while the shape factor decreased. This can be explained by considering an increase in the impact energy between the droplet and the substrate due to an increased droplet velocity.[48]

The properties of an ink droplet can also be influenced by electrical signals such as the input voltage and pulse width during ink-jet printing using a piezoelectric print head. Fig. 7 and 8 show the printability characteristics of the aqueous ceramic ink when the input voltage of the print head was 70, 80, and 90 V, and the pulse width was fixed at 8 μs. The droplet velocity and tail length increased upon increasing the input voltage, since the volumetric deformation of the piezoelectric actuator and the jetting pressure increased with the input voltage.[49] In addition, the printed dot area of the aqueous ceramic ink increased at higher input voltages, and the highest shape factor was obtained at an input voltage of 80 V.

The effect of the pulse width was then examined, as outlined in Fig. 9 and 10. With a fixed input voltage of 80 V, an increase in the pulse width from 6 to 8 μs resulted in increases in both the droplet velocity and the tail length. However, upon increasing the pulse width further to 10 μs, the droplet velocity and tail length decreased, thereby indicating that a pulse width of 8 μs was optimal for printing of the aqueous ceramic ink on the ceramic tile.

Conclusions

We herein reported the preparation of an eco-friendly aqueous ceramic ink for ink-jet printing based on the use of a thermally stable yellow ceramic pigment. The yellow ceramic pigment based on the Pr-$ZrSiO_4$ structure was micronized into the suitable particle size for inkjet printing that the average particle size is under 300 nm in diameter. A graft polymer was introduced as a surfactant to improve the dispersion stability of the ceramic pigments in aqueous ink. Polyacrylic acid (PAA) was employed as the main chain to impart electrostatic repulsion, and poly(ethylene glycol) methyl ether methacrylate (PMEM) was grafted as the side chain to give steric hindrance. The optimized concentration of the graft polymer which is revealed using the viscosity measurement was 0.5 mg m^{-2}. The sedimentation velocity of the pigments was lowered by 55% compared with the

use of PAA alone as a surfactant, and foaming was significantly reduced. Furthermore, the jettability and printability of the aqueous ceramic ink were optimized by adjusting the rheological properties of the ink and the operation conditions of the piezoelectric print head, which in turn affected the shape, velocity, and tail length of the resulting ink droplets. The optimal rheological properties of the aqueous ceramic ink were shown when the concentration of the thickener was 15 wt%. The introduction of an adequate flow resistance through thickener addition also improved the jettability and printability of the ink. Also, the optimized values of the pulse width and the voltage were 80 V and 8 μs, respectively. These results are of importance due to the ongoing necessity for novel eco-friendly and functional ceramic inks to replace organic-containing solvent-based ink-jet printing inks for application in the ceramic tile decoration industry.

Conflicts of interest

There are no conflicts to declare.

References

1 S. D. Hoath, *Fundamentals of inkjet printing: the science of inkjet and droplets*, John Wiley & Sons, New Jersey, 2016.
2 J. Stringer and B. Derby, *Langmuir*, 2010, **26**, 10365–10372.
3 J. Li, F. Rossignol and J. Macdonald, *Lab Chip*, 2015, **15**, 2538–2558.
4 D. J. Hayes, W. R. Cox and M. E. Grove, *J. Soc. Inf. Disp.*, 2001, **9**, 9–13.
5 A. Capasso, A. D. R. Castillo, H. Sun, A. Ansaldo, V. Pellegrini and F. Bonaccorso, *Solid State Commun.*, 2015, **224**, 53–63.
6 C. Zanelli, G. L. Güngör, A. Kara, M. Blosi, D. Gardini, G. Guarini and M. Dondi, *Ceram. Int.*, 2015, **41**, 6507–6517.
7 G. Ferrari and P. Zannini, *Bol. Soc. Esp. Ceram. Vidrio*, 2017, **56**, 226–236.
8 A. S. Roy, M. Bhattacharjee, R. Mondal and S. Ghosh, *J. Oleo Sci.*, 2007, **56**, 623–628.
9 Z. Pan, Y. Wang, H. Huang, Z. Ling, Y. Dai and S. Ke, *Ceram. Int.*, 2015, **41**, 12515–12528.
10 A. Soleimani-Gorgani, M. Ghahari and M. Peymannia, *J. Eur. Ceram. Soc.*, 2015, **35**, 779–786.
11 N. Reis, C. Ainsley and B. Derby, *J. Appl. Phys.*, 2005, **97**, 094903.
12 B. V. Antohe and D. B. Wallace, *J. Imaging Sci. Technol.*, 2002, **46**, 409–414.
13 A. Friederich, J. R. Binder and W. Bauer, *J. Am. Ceram. Soc.*, 2013, **96**, 2093–2099.
14 S. Magdassi, *The chemistry of inkjet inks*, World Scientific, Singapore, 2009.
15 D. Gardini, M. Blosi, C. Zanelli and M. Dondi, *J. Nanosci. Nanotechnol.*, 2015, **15**, 3552–3561.
16 J. R. Castrejon-Pita, W. R. S. Baxter, J. Morgan, S. Temple, G. D. Martin and I. M. Hutchings, *Atomization Sprays*, 2013, **23**, 541–565.
17 Y. Marinova, J. M. Hohemberger, E. Cordoncillo, P. Escribano and J. B. Carda, *J. Eur. Ceram. Soc.*, 2003, **23**, 213–220.
18 R. A. Eppler, *J. Am. Ceram. Soc.*, 1970, **53**, 457–462.
19 M. Trojan, *Dyes Pigm.*, 1990, **13**, 281–287.
20 G. H. Zhang, N. Zhu, Y. B. Li, J. F. Zhu, Y. R. Jia and L. Ge, *Fuel Process. Technol.*, 2017, **161**, 1–7.
21 G. Cummins, R. Kay, J. Terry, M. P. Desmulliez and A. J. Walton, In *IEEE 13th Electronics Packaging Technology Conference*, 2011, pp. 256–261.
22 R. I. Tomov, M. Krauz, J. Jewulski, S. C. Hopkins, J. R. Kluczowski, D. M. Glowacka and B. A. Glowacki, *J. Power Sources*, 2010, **195**, 7160–7167.
23 D. Rosslere, *Developments in ceramic materials research*, Nova Science Publishers, New York, 2007.
24 M. Shoyama, H. Nasu and K. Kamiya, *J. Ceram. Soc. Jpn.*, 1998, **106**, 279–284.
25 M. Lejeune, T. Chartier, C. Dossou-Yovo and R. Noguera, *J. Eur. Ceram. Soc.*, 2009, **29**, 905–911.
26 D. Kuscer, G. Stavber, G. Trefalt and M. Kosec, *J. Am. Ceram. Soc.*, 2012, **95**, 487–493.
27 C. P. Whitby, P. J. Scales, F. Grieser, T. W. Healy, G. Kirby, J. A. Lewis and C. F. Zukoski, *J. Colloid Interface Sci.*, 2003, **262**, 274–281.
28 J. A. Lewis, H. Matsuyama, G. Kirby, S. Morissette and J. F. Young, *J. Am. Ceram. Soc.*, 2000, **83**, 1905–1913.
29 G. H. Kirby and J. A. Lewis, *J. Am. Ceram. Soc.*, 2004, **87**, 1643–1652.
30 R. L. Hoffman, *Trans. Soc. Rheol.*, 1972, **16**, 155–173.
31 W. H. Boersma, J. Laven and H. N. Stein, *J. Colloid Interface Sci.*, 1992, **149**, 10–22.
32 H. M. Laun, R. Bung, S. Hess, W. Loose, O. Hess, K. Hahn, E. Hadicke, R. Hingmann, F. Schmidt and P. Lindner, *J. Rheol.*, 1992, **36**, 743–787.
33 S. Khandavalli and J. P. Rothstein, *J. Rheol.*, 2014, **58**, 411–431.
34 T. G. Mezger, *Applied rheology: with joe flow on rheology road*, Anton Paar, Austria, 2014.
35 N. Mandzy, E. Grulke and T. Druffel, *Powder Technol.*, 2005, **160**, 121–126.
36 D. H. Everett, *Basic principles of colloid science*, The Royal Society of chemistry, London, 1988.
37 R. K. Pujala, *Dispersion stability, microstructure and phase transition of anisotropic nanodiscs*, Springer, Berlin, 2014.
38 J. K. Lim, S. A. Majetich and R. D. Tilton, *Langmuir*, 2009, **25**, 13384–13393.
39 H. K. Mahabadi and A. Rudin, *Makromol. Chem.*, 1978, **179**, 2977–2988.
40 K. Yoshioka, E. Sakai, M. Daimon and A. Kitahara, *J. Am. Ceram. Soc.*, 1997, **80**, 2667–2671.
41 D. Jang, D. Kim and J. Moon, *Langmuir*, 2009, **25**, 2629–2635.
42 W. L. Zhang, H. J. Choi, H. S. Ko and K. S. Kwon, *J. Ind. Eng. Chem.*, 2015, **22**, 120–126.
43 K. A. M. Seerden, N. Reis, J. R. G. Evans, P. S. Grant, J. W. Halloran and B. Derby, *J. Am. Ceram. Soc.*, 2001, **84**, 2514–2520.
44 B. Derby, *Annu. Rev. Mater. Res.*, 2010, **40**, 395–414.

45 H. C. Nallan, J. A. Sadie, R. Kitsomboonloha, S. K. Volkman and V. Subramanian, *Langmuir*, 2014, **30**, 13470–13477.
46 M. Özkan, K. Dimic-Misic, A. Karakoc, S. G. Hashmi, P. Lund, T. Maloney and J. Paltakari, *Org. Electron.*, 2016, **38**, 307–315.
47 E. D. Wilkes, S. D. Phillips and O. A. Basaran, *Phys. Fluids*, 1999, **11**, 3577–3598.
48 C. Clanet, C. Béguin, D. Richard and D. Quéré, *J. Fluid Mech.*, 2004, **517**, 199–208.
49 H. C. Wu, T. R. Shan, W. S. Hwang and H. J. Lin, *Mater. Trans.*, 2004, **45**, 1794–1801.

